(Preprint) AAS 20-121

SIMULTANEOUS AND DISTINCT VISIBLE AND THERMAL RADIATION PRESSURE DYNAMICS

Scott J.K. Carnahan[*], Hanspeter Schaub[†]

This work modifies previously published methods to evaluate solar radiation pressure (SRP) and thermal radiation pressure (TRP) dynamic effects on a spacecraft and extends these models to incorporate self-emitted TRP. The modifications delineate effects due to visible-band and thermal-band radiation. With these methods, the independent effects of thermal and visible spectrum radiation on spacecraft orbits can be analyzed using only a small number of coefficients. The effects captured include dynamics due to visible and thermal solar radiation, earth albedo, earth infrared radiation, and spacecraft thermal emissions. Spacecraft thermal control systems rely on surface finishes with specified solar absorptance and thermal emittance coefficients. These coefficients couple the spacecraft thermal design with spacecraft dynamics via radiation pressure. This work analyzes that coupling by closely examining how the application of the coefficients in the visible and thermal spectral bands affects orbit propagation. Finally, numerical modeling tools are developed that allow for the analysis of thermo-physical models of spacecraft tightly coupled to the spacecraft dynamics and environment. Together, the work here forms the basis for the analysis of the full, spectral analysis of radiation pressure on spacecraftr trajectories.

INTRODUCTION

Radiation pressure effects on spacecraft are only becoming more important in mission design, particulary those missions with ultra precision orbit knowledge requirements. Examples of such missions include TOPEX/Poseidon, GRACE, and Rosetta.[1][2][3] Scheeres developed Fourier transform methods to analyze the effects of SRP on asteroids.[4] McMahon expanded this work to study SRP effects on spacecraft.[5] Hesar further built on that work to study the dynamical effects of thermal irradiance on a spacecraft.[6] In this paper, the SRP models and TRP models are applied simultaneously with a thermal self-emission model to a spacecraft in orbit about Earth. With the assumption of a controlled and Earth-facing spacecraft, self-emitted radiation pressure is also Fourier transformed as a function of solar longitude in the body frame. Because heating of the spacecraft due to internal components is considered, a further assumption of nominal operations is made. In applying the combination of these models to assess the thermal and visible band radiation pressure effects, care is taken to properly account for the interaction of the radiant spectrum and the surface property coefficients used.

In practice, engineers apply solar absorptance values to the full magnitude of solar flux. Even while holding solar absorptance constant, thermal engineers may vary surface finish emittance values to their extent between 0 and 1. Because absorptance values are measured only over about 95%

[*]Engineer, Cesium, 13412 Galleria Circle, Suite H-100, Austin, TX, 78738

[†]Professor and Glenn L. Murphy Endowed Chair, Aerospace Engineering Sciences, CU Boulder, 3775 Discovery Dr, Boulder, CO, 80303

of the solar spectrum, there is a dynamical and thermal effect of solar irradiance that is lost in this analysis.[7] The extent of this effect is investigated to characterize its impact on orbit prediciton.

As in previous work, the derivation here depends on the fact that radiation pressure forces are intrinsically tied to body-fixed properties [McMahon top of page 1420]. Furthermore, the necessary assumptions are made regarding orbit, attitude, and operations such that the radiation pressure forces repeat each orbit for a given position of Earth in its heliocentric orbit. For SRP models, this means that the forces need to be a function of the sun heading vector. For planetary infrared emissions, this means that the force needs to be a function of the facet heading direction from the spacecraft for each planet facet. More generally, given the right orbit and attiude assumptions, the radiation pressure needs to be written as a function of the spacecraft heading to the source of radiation, which will be referred to as $\hat{u}$ regardless of if the source is the sun or a facet on the surface of Earth.

FORCE DEFINITIONS

The five forces of interest are radiation pressure due to visible solar irradiance, infrared solar irradiance, visible albedo, Earth infrared irradiance, and spacecraft self-emitted infrared radiation. Earth-reflected infrared radiation is assumed to be a smaller effect. The force models follow from McMahon and Hesar, but vary in a few key ways. First, all notation from Hesar is converted to the same dyad notation used by McMahon for consistency. Second, both McMahon and Hesar derive force models that account for some combination of visible and infrared radiation. Here, the distinction between visible and thermal radiation is made explicit.

Visible Solar Radiation Pressure

$$\boldsymbol{F}_{SRP,v} = P_v(R) \sum_{i=1}^{N} f_{i,v}(\hat{\boldsymbol{u}}) \tag{1}$$

where the subscript v is added to indicate that this equation accounts only for visible spectrum irradiance. Further,

$$P_v(R) = \frac{G_{1,v}}{R^2} \tag{2}$$

where $G_{1,v}$ is the visible portion of the solar constant and

$$f_{i,v} = -[\underbrace{\{\rho_{i,v} s_{i,v}(2\hat{\boldsymbol{n}}_i\hat{\boldsymbol{n}}_i - \overline{\overline{U}}) + \overline{\overline{U}}\} \cdot \hat{\boldsymbol{u}}_s\hat{\boldsymbol{u}}_s \cdot \hat{\boldsymbol{n}}_i}_{\text{specular reflection}} + \underbrace{\frac{2}{3}(1 - s_{i,v})\rho_{i,v}\hat{\boldsymbol{n}}_i\hat{\boldsymbol{n}}_i \cdot \hat{\boldsymbol{u}}_s}_{\text{diffuse reflection}}]H_i(\hat{\boldsymbol{u}}_s)A_i. \tag{3}$$

$\overline{\overline{U}}$ is the identity dyad. The total reflectivity $\rho_{i,v}$ and $s_{i,v}$ is the fraction of the reflected light which is reflected specularly. Spacecraft surface facet normal vectors are written $\hat{\boldsymbol{n}}_i$. The sun heading vector from the spacecraft is $\hat{\boldsymbol{u}}_s$. H_i is the spacecraft surface facet sun visiblity factor, which is 1 if the sun is visible to the facet and 0 otherwise. A_i is the facet surface area. Note that perfect Lambertian diffuse reflection has been assumed and thermal re-radiation is not included here. Finally, note that

$$\rho_{i,v} = 1 - \alpha_i \tag{4}$$

where α_i is the solar absorptance value of surface facet i and the fraction of the irradiance that is spectrally reflected is ρs, regardless of the spectral band.

Infrared Solar Radiation Pressure A portion of the solar spectrum lies at wavelengths higher than those at which solar absorptance values are typically measured and calculated. This portion is treated separately here. In such case, the infrared SRP is calculated as

$$\boldsymbol{F}_{SRP,I} = P_I(R) \sum_{i=1}^{N} f_{i,I}(\hat{\boldsymbol{u}}) \tag{5}$$

$$P_I(R) = \frac{G_{1,I}}{R^2} \tag{6}$$

$$f_{i,I} = -[\underbrace{\{\rho_{i,I} s_{i,I}(2\hat{\boldsymbol{n}}_i\hat{\boldsymbol{n}}_i - \overline{\overline{U}}) + \overline{\overline{U}}\} \cdot \hat{\boldsymbol{u}}_s\hat{\boldsymbol{u}}_s \cdot \hat{\boldsymbol{n}}_i}_{\text{specular reflection}} + \underbrace{\frac{2}{3}(1 - s_{i,I})\rho_{i,I}\hat{\boldsymbol{n}}_i\hat{\boldsymbol{n}}_i \cdot \hat{\boldsymbol{u}}_s}_{\text{diffuse reflection}}]H_i(\hat{\boldsymbol{u}}_s)A_i. \tag{7}$$

where all subscripts v have been replaced with I to indicate the thermal infrared spectral band. Finally,

$$\rho_{i,I} = 1 - \epsilon_i \tag{8}$$

where ϵ_i is the thermal emittance of the surface facet i.

Spacecraft Thermal Emission For the purposes of this work, the spacecraft thermal systems are assumed to operate at some constant power dissipation. In that case, the heat emitted by any part of the spacecraft is dependent on the irradiance on the spacecraft. For the simplest case, this will depend only on solar irradiance and albedo, both of which are functions of the sun heading from the spacecraft. In this case, the thermal self emittance radiation pressure (SERP) can be written as

$$F_{SERP} = \frac{2\sigma}{3c} \sum_{i=1}^{N} A_i T_i^4(\hat{\boldsymbol{u}}_s)\epsilon_i\hat{\boldsymbol{n}}_i \tag{9}$$

where the $\frac{2}{3}$ factor comes from integrating in space over a Lambertian emitter, σ is the Stephan-Boltzmann constant, A_i is the surface area of the facet, $T(\hat{\boldsymbol{u}}_s)_i$ is the absolute temperature of the facet which depends on the sun heading, c is the speed of light, and $\hat{\boldsymbol{n}}_i$ is the surface normal of the facet. $T(\hat{\boldsymbol{u}}_s)_i$ can also be made to depend on spacecraft intneral systems thermal, if that thermal performance is cyclical over an orbit.

Earth Albedo Hesar's model actually covers both albedo and planetary emission, so it is dissected here into separate visible and thermal effects. This model is based on a meshed planet surface. For simplicity, here we assume uniform surface properties across the planet to calculate F_{Alb}, the radiation pressure force due to Earth-reflected radiation from the sun.

$$F_{Alb} = \frac{P_v(R)}{c\pi} \sum_{j\in\mathcal{K}} P_{j,v} \sum_{i=1}^{N} f_{ij} \tag{10}$$

where

$$P_{j,v} = a_j \frac{A_j}{u_j^2} H_j(\hat{\boldsymbol{u}}_s)\hat{\boldsymbol{n}}_j \cdot \hat{\boldsymbol{u}}_s\hat{\boldsymbol{n}}_j \cdot \hat{\boldsymbol{u}}_j \tag{11}$$

assumes pure specular reflection from the planet and

$$f_{ij,v} = -[\{\rho_{i,v} s_{i,v}(2\hat{\boldsymbol{n}}_i\hat{\boldsymbol{n}}_i - \overline{\overline{U}}) + \overline{\overline{U}}\} \cdot \hat{\boldsymbol{u}}_j\hat{\boldsymbol{u}}_j \cdot \hat{\boldsymbol{n}}_i + \frac{2}{3}(1 - s_{i,v})\rho_{i,v}\hat{\boldsymbol{n}}_i\hat{\boldsymbol{n}}_i \cdot \hat{\boldsymbol{u}}_j]H_i(\hat{\boldsymbol{u}}_j)A_i. \tag{12}$$

Additionally, $H_i(\hat{\boldsymbol{u}}_j)$ is the the sun-visibility function of the surface element j, a_j is the albedo of the surface element, c is the speed of light, and A_j is the surface area of element j. The sun heading from the planet is $\hat{\boldsymbol{u}}_s$ and the heading from a planet surface element to the spacecraft is $\hat{\boldsymbol{u}}_j$.

Earth Infrared Radiation Note that thermal spectrum light reflected by the planet (thermal albedo) is ignored. The radiation pressure force from the planet is denoted PIR (planetary infrared)

Here, the light coming from the planet is due to thermal emission, so we have

$$F_{\mathrm{PIR}} = \sum_{j \in \mathcal{K}} P_{j,I} \sum_{i=1}^{N} f_{ij,I} \tag{13}$$

where

$$f_{ij,I} = -[\{\rho_{i,I} s_{i,I}(2\hat{\boldsymbol{n}}_i\hat{\boldsymbol{n}}_i - \overline{\overline{U}}) + \overline{\overline{U}}\} \cdot \hat{\boldsymbol{u}}_j\hat{\boldsymbol{u}}_j \cdot \hat{\boldsymbol{n}}_i + \frac{2}{3}(1 - s_{i,I})\rho_{i,I}\hat{\boldsymbol{n}}_i\hat{\boldsymbol{n}}_i \cdot \hat{\boldsymbol{u}}_s]H_i(\hat{\boldsymbol{u}}_j)A_i. \tag{14}$$

and $P_{j,I}$ is the emission function of the surface facet j. $P_{j,I}$ is a function of the absolute effective surface temperature which is taken to be constant for the time being.

$$P_{j,I} = \sigma A_j \epsilon_j T_j^4. \tag{15}$$

Total Visible and Thermal Forces Now, the force models above can be combined to find solutions for the total radiation pressure in each of the visible and thermal bands. The total radiation pressure force, F_{RP} is

$$F_{RP} = F_{RP_v} + F_{RP,I} \tag{16}$$

where

$$F_{RP_v} = F_{SRP,v} + F_{Alb} \tag{17}$$

and

$$F_{RP,I} = F_{SRP,I} + F_{SERP} + F_{PIR} \tag{18}$$

With the above definitions, a quasi-analytical predictin of the secular effects of radiation pressure on a trajectory can be investigated which accounts independently for visible and thermal band radiation, both reflected and self-emitted.

A DETAILED LOOK AT SOLAR ABSORPTANCE

Spacecraft thermal surface finishes are specified in terms of solar absorptance, α, and thermal emittance, ϵ. Each coefficient can be between 0 and 1 and real materials can yield almost any combination of the two. A lazy statement of Kirchoff's law of thermal radiation is "For an arbitrary body emitting and absorbing thermal radiation in thermodynamic equilibrium, the emissivity is equal to the absorptivity"*. That statement can lead, at first glance, to confusion as to the definition of absorptance and emittance, so it is important to clarify that absortance and emittance describe the same physical property of a surface, but in difference wavelength bands. Absorptance is specified over most of the solar spectrum while emittance is focused over the peak of black bodies radiating at "normal" temperatures.

*https://en.wikipedia.org/wiki/Kirchhoff%27s_law_of_thermal_radiation

Absorptance is generally taken to be the mean percentage of absorption of the solar irradiance on the surface. Mathematically, this would be written as

$$\alpha = \frac{\int_0^\infty \alpha(\lambda)H(\lambda)d\lambda}{\int_0^\infty H(\lambda)d\lambda} \tag{19}$$

where H is the spectral irradiance from the sun at Earth (not modified by the atmosphere). In reality, absorptance is measured and calculated in a laboratory, where the irradiance is likely to be approximated by a black body and the spectrum is limited, so that

$$\alpha = \frac{\int_a^b \alpha(\lambda)H(\lambda)d\lambda}{\int_a^b H(\lambda)d\lambda} \tag{20}$$

with a being some lower limit on the wavelength and b an upper limit. ASTM specifies that tests for solar absorptance cover the spectral range from $500\mu m - 2500\mu m$.[8]

Likewise, emittance is intended as the mean over the emitted spectrum from a surface[7*]

$$\epsilon = \frac{\int_0^\infty \alpha(\lambda)E(\lambda)d\lambda}{\int_0^\infty HE\lambda)d\lambda} \tag{21}$$

where E is the spectral emissivity of the surface. Again, like absorptance, emissivity is approximated in the laboratory by the use of a limited spectrum so that in reality

$$\epsilon = \frac{\int_c^d \alpha(\lambda)E(\lambda)d\lambda}{\int_c^d HE\lambda)d\lambda} \tag{22}$$

So, when combining ϵ and α it is desirable for c to be as close to and greater than b in order to have a clear assignment of spectral regions to coefficients. When mentioned, the spectrum over which the emittance is measured varies greatly.,[79]

Henninger's solar absorptance coefficients were calculated from 300nm to 2400nm with the understanding that this covers 95% of the solar spectrum.[7] Assuming that the thermal emittance value, ϵ, provides a better average value for the remaining 5% of the spectrum, some analysis can be done.

In general, the solar absorptance is applied to the solar flux, S, to get the incident radiation power, P as

$$P = S\alpha A \tag{23}$$

where A is the effective area of some surface (modified by the cosine to the solar vector and any view factors). If, instead, the solar irradiance is distributed into visible and thermal bands this incident power is written

$$P = SA(f_v\alpha + f_I\epsilon) \tag{24}$$

where f_v is the fraction of the spectrum in the visible band and f_I is $1 - f_v$, the fraction of the spectrum in the infrared band. Now we can understand the impact of the typical method of applying equation 23. As seen in fig. 1, the variation due to using a banded spectrum is strongest when the solar absorptance is low and the thermal emittance is high and this variation is over 40% of teh

*Modern ASTM standard tests for emissivity[9] generally utilitize an aparatus that measure the integrated emissivity directly, rather than taking spectral measurements.

standard method for calculating flux. This considers an α as low as 0.1 and an ϵ as high as 1.0. The trend is evident when observing the ratio mathematically as

$$R = \frac{f_v \alpha + f_I \epsilon}{\alpha} \tag{25}$$

This sort of low-α, high-ϵ configuration is physical and plausible for "white paints and second-surface mirrors".[10]

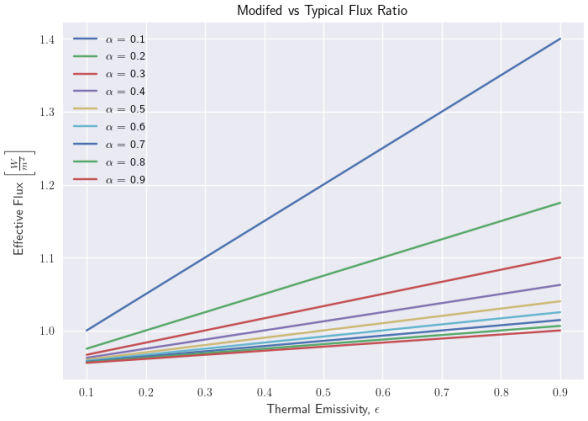

Figure 1. The ratio of the flux calculated with a discretized solar spectrum over the standard method using only solar absorptance.

THERMAL SURFACE SRP EXTREMA

The above analysis covers the effects of α and ϵ on absorbed radiation, but this does not show how those coefficients affects the forces due to impinging and reflected photons. To investigate this, eq. (3), is manipulated to isolate the effects of absortance in a given band for the cases of pure specular and pure diffuse reflection. In this analysis, α will be used to reference the absorptance, regardless of the spectral band. Furthermore, in the diffuse case, s, the specular portion of reflected light, is 0 while it is 1.0 in the specular case. In that case, $\rho s = \rho$. Finally, recall that $1 - \rho = \alpha$. Now, SRP is investigated by looking only at eq. (3) because this term alone captures the pertinent information for relative comparisons.

Pure Diffuse Reflection

In eq. (3), the specular terms not multiplied by the reflectivity account for the pressure due to impinging radiation brought to a stop on the surface. Therefore, for a single panel, those terms remain in the diffuse case and we are left with:

$$\frac{f}{A} = -[\hat{\boldsymbol{u}}_s \hat{\boldsymbol{u}}_s \cdot \hat{\boldsymbol{n}} + \frac{2}{3}(1-\alpha)\hat{\boldsymbol{n}}\hat{\boldsymbol{n}} \cdot \hat{\boldsymbol{u}}_s]. \tag{26}$$

H has been dropped because unlit facets are not interesting. This is expanded to isolate α.

$$\frac{f}{A} = -\hat{\boldsymbol{u}}_s \hat{\boldsymbol{u}}_s \cdot \hat{\boldsymbol{n}} - \frac{2}{3}\hat{\boldsymbol{n}}\hat{\boldsymbol{n}} \cdot \hat{\boldsymbol{u}}_s + \alpha \hat{\boldsymbol{n}}\hat{\boldsymbol{n}} \cdot \hat{\boldsymbol{u}}_s \tag{27}$$

This can be further simplified by replacing the dot products with cosines.

$$\frac{f}{A} = -(\hat{\boldsymbol{u}}_s + \frac{2}{3}\hat{\boldsymbol{n}})\cos\theta + \alpha\cos\theta\hat{\boldsymbol{n}} \tag{28}$$

If $\hat{\boldsymbol{u}}_s$ and $\hat{\boldsymbol{n}}$ are the same direction, then it reduces further to

$$\frac{f}{A} = -\frac{5}{3}\hat{\boldsymbol{n}} - \alpha\hat{\boldsymbol{n}} \tag{29}$$

Pure Specular Reflection

For pure specular reflection, the diffuse term is removed entirely, leaving on the impinging and specularly reflecting terms.

$$\frac{f}{A} = -(1-\alpha)(2\hat{\boldsymbol{n}}_i\cos^2\theta + \hat{\boldsymbol{u}}_j\cos\theta) - \hat{\boldsymbol{u}}_j\cos\theta \tag{30}$$

which can be simplified further to separate α.

$$\frac{f}{A} = -2\cos\theta(\hat{\boldsymbol{n}}_i\cos\theta + \hat{\boldsymbol{u}}_j) - \alpha(2\hat{\boldsymbol{n}}_i\cos^2\theta + \hat{\boldsymbol{u}}_j\cos\theta) \tag{31}$$

and taking the sun heading to be the same as the surface normal

$$\frac{f}{A} = -(4+3\alpha)\hat{\boldsymbol{n}}\hat{\boldsymbol{n}} \tag{32}$$

NUMERICAL MODELING

While the previous sections provide analytical insight into the effects of independently modeled thermal and visible radiation pressure, it is desirable to have a numerical tool which can predict these effects in less idealized situations. This requires a full thermo-physical model of the spacecraft under study. To this end, a thermal physics library has been developed for Basilisk * which allows for the full coupling of thermal modeling to spacecraft attitude and trajectory simulation, including all relevant environmental radiation sources.

Mathematical Model

The thermal modeling library is developed as a Finite Difference Modeling library. This method approximates the continuous nature of of heat transfer with a model based on the temperature difference across an element. Whereas Fourier's law is written in the continuous differential form for a point in a solid as

$$\boldsymbol{q} = -C\nabla T, \tag{33}$$

a finite difference approximation would say that

$$q = C\Delta T \tag{34}$$

*http://hanspeterschaub.info/basilisk/index.html

where q is the heat flow in one direction through the solid, ΔT is the difference in temperature from one end of the solid to the other, and C is the conductance. Finite difference models are usually coupled with other simplifying assumptions as well. For instance, with a heat flow through a rod, one may assume heat flows only axially and that there is no radiation out from the rod. Then, if radiation analysis is desired, this may be added on as a separate model. This allows for the combination of well known and well behaved analytical solutions to heat transfer in complex geometry. Finite difference modeling is well known and widely used in spacecraft thermal analysis since at least the 1950s. Today, the best known tool for spacecraft thermal analysis, Thermal Desktop, is built on SINDA, which is a Finite Difference solver, although many people unfamiliar with it assume it is a Finite Element solver because of the complex geometry seen in images of results of this analysis.[11] That is to say that despite the underlying mathematics of the finite difference method being simple, the combination of many of such elements can yield both interesting and accurate results.

Numerical Propogation

The library built into Basilisk provides for transient forward propogation of temperature via Euler integration. This method was chosen because transient solutions are desired and Euler integration is naturally available within Basilisk. Also, if attitude dynamics are being modeled, the time step of the simulation is likely to be smaller than that needed for thermal dynamics. This scheme allows entirely for algorithmic decoupling of the various thermal models via the Basilisk messaging system because no additional information needs to be tightly coupled to an integrator or solver. Each thermal mass node calculates the net heat rate at that node and propagates its own temperature forward in time.

The only exception to the forward propagation is the Arithmetic Surface model. This model solves a surface to the temperature required for thermal equilibrium at each time step. It is a common model for thin surfaces with low thermal inertia such as thermal surface finish films. Such a model is similar to that commonly used in radiation pressure analyses, but these surfaces are not necessarily used to model the entire exterior of a spacecraft in this work. Additionally, more heat can be directed from the interior of the spacecraft to one of these surfaces models, causing it to radiate more than it would in other analyses. For example, heat could be generated internally due to batteries or reaction wheels and the explusion of this heat can be captured here.

Mathematical Description

The thermal library is split into a set of models which are connected by Basilisk messages to form a thermal heat transfer network. There is not a realistic limit on the heat transfer models that can be developed in the basilisk library, but only a handful are needed as building blocks to a reasonably high fidelity thermal model of a spacecraft in orbit. The initial models needed are

- arithmetic surface

  The arithmetic surface balances the temperature of a surface to equilibrium via thermal emission. The user inputs the thermal emittance and surface area. Additionally, all other input heat sources are connected via message. The mathematical formulation of this model is

  $$T = \sqrt[4]{\frac{\sum \dot{q}}{\epsilon A \sigma}} \tag{35}$$

  where Σq is the sum of the input heat rates, ϵ is the thermal emittance of the surface, A is the effective surface area of the element, σ is the Stefan-Boltzmann constant, and T is the temperature at which the surface radiates in thermal equilibrium.

- conductor

  The conductor is the most basic building block of most thermal networks. Upstream (T_u) and downstream (T_d) temperature nodes are connected via message and this model follows the form

  $$q = C\Delta T \tag{36}$$

  where C is the conductance in $\frac{W}{K}$, $\Delta T = T_u - T_d$, and q is the heat rate across the conductor.

- emitter

  The emitter follows the Stefan-Boltzmann law and is connected only to an upstream mass temperature via message. The Stefan Boltzmann law for a grey body is

  $$q = \sigma A \epsilon T^4 \tag{37}$$

  where σ is the Stefan-Boltzmann consant, A is the effective emitting surface area, ϵ is the thermal emittance of the surface, and T is the upstream temperature. The emitter model is used in combination with the flux heating model (below) to account for all exchange with the environment rather than calculating the net exchange between the spacecraft surface and the Earth (for instance) using view factors.

- flux heating

  The flux heating model requires knowledge (via messages) of the spacecraft attitude, the flux source heading, and the flux magnitude at the spacecraft. The formulation for heating via flux source is

  $$q = \hat{\boldsymbol{n}} \cdot \hat{\boldsymbol{s}} F A \alpha \tag{38}$$

  where q is the heat into the surface, $\hat{\boldsymbol{n}}$ is the surface unit normal in the spacecraft body frame, $\hat{\boldsymbol{s}}$ is the source unit heading in the body frame, F is the flux magnitude along the source heading, A is the area of the surface, and α is the absorptance of the surface in the relevant spectral band. For instance, α indicates the absorptance in the thermal band (usually known as ϵ) if the flux heating being modeled is heating due to earth infrared emissions.

- heat source

  The heat source model applies a constant heat source as specified by the user. A thermal mass attached to this model receives that heat rate. The user can stop the simulation to change this heat rate.

  $$q = q_{\text{user}} \tag{39}$$

- mass

  Thermal masses perform the basic Euler integration of heat rates to propagate the temperatures in the system forward in time according to

  $$\dot{T} = \frac{\sum q}{m c_p} \tag{40}$$

  where $\dot{T}$ is the instantaneous temperature rate, $\sum q$ is the sum of all heat rates into the node, m is the mass of the node, and c_p is the specific heat of the material the node is modeling. Then, the change in temperature is calculated as

  $$\Delta T = \dot{T} \Delta t \tag{41}$$

  and the temperature is updated.

- radiation conductor

  The radiation conductor calculates nonlinear heat flow between two thermal masses as a function of surface properties of flat surfaces by calculating an equivalent conduction at each point according to

$$C = \sigma A f \frac{T_u^3 + T_u T_d^2 + T_u^2 T_d + T_d^3}{\frac{1}{\epsilon_u} + \frac{1}{\epsilon_d} - 1} \tag{42}$$

  where C is the equivalent conuctance, A is the area (assuming each surface has equal area), f is the view factor between the surfaces, T_u is the upstream temperature, T_d is the downstream temperature, ϵ_u is the upstream surface emittance, and ϵ_d is the downstream surface emittance. The conductance is then used to calculate the heat rate as with the linear conductor model. The radiation conductor is a useful model for internal radiation heat transfer in situations where radiation is comparable or much greater than the heat transfered via conductance. If the temperatures of both the up and downstream nodes stay fairly constant throughout a simulation, it is more efficient to calculated C ahead of time and used a standard linear conduction model instead.

Heat Flow Convention

In building a thermal heat rate network, it is important to be clear and consistent with sign conventions. In this library, heat paths are connected to "upstream" and "downstream" temperature nodes. Heat flow across a conductor is then considered positive if flowing from upstream to downstream. Emitter models are only connected to upstream temperature nodes and the heat flow is always positive.

On the other hand, for thermal mass nodes, heat flow is considered positive *into* the node and negative *out of* the node. Therefore, if a path is connected as an "upstream" path and has a positive heat rate, that heat will increase the temperature of the mass node. On the other hand, if a node is a connected to a "downstream" path that has a negative heat rate, this will also increase the temperature of the node.

A CAPABLE AND FLEXIBLE SOLUTION FOR RADIATION PRESSURE DYNAMICS

Radiation pressure dynamics have played important roles in spacecraft trajectories. They also have the potential to be even more influential in future missions. As such, it is important to continue to develop both numerical and analytical tools to study these dynamics. Analytical forms have been presented which detail the distinct effect of thermal and visible band radiation, both incoming and outgoing. The surface properties commonly used in this sort of analysis have been examined in detail. A capable library of numerical tools for modeling dynamics-coupled spacecraft thermophysics has been developed. Although each analysis may call for unique thermal models or integration techniques, this work forms a basis from which a more complete radiation pressure analysis can be done, including spacecraft operations and self-emission.

REFERENCES

[1] J. A. Marshall and S. B. Luthcke, "Modeling radiation forces acting on Topex/Poseidon for precision orbit determination," *Journal of Spacecraft and Rockets*, Vol. 31, Jan. 1994, pp. 99–105, 10.2514/3.26408.

[2] E. Fahnestock, R. Park, D.-N. Yuan, and A. Konopliv, "Spacecraft Thermal and Optical Modeling Impacts on Estimation Of the GRAIL Lunar Gravity Field," *AIAA/AAS Astrodynamics Specialist Conference*, Minneapolis, Minnesota, American Institute of Aeronautics and Astronautics, Aug. 2012, 10.2514/6.2012-4428.

[3] Y. Sugimoto, J. v. d. Ha, and B. Rievers, "Thermal Radiation Model for the Rosetta Spacecraft," *AIAA/AAS Astrodynamics Specialist Conference*, Toronto, Ontario, Canada, American Institute of Aeronautics and Astronautics, Aug. 2010, 10.2514/6.2010-7659.

[4] D. Scheeres, "The dynamical evolution of uniformly rotating asteroids subject to YORP," *Icarus*, Vol. 188, June 2007, pp. 430–450, 10.1016/j.icarus.2006.12.015.

[5] J. W. McMahon and D. J. Scheeres, "New Solar Radiation Pressure Force Model for Navigation," *Journal of Guidance, Control, and Dynamics*, Vol. 33, Sept. 2010, pp. 1418–1428, 10.2514/1.48434.

[6] S. G. Hesar, D. J. Scheeres, J. W. McMahon, and B. Rozitis, "Precise Model for Small-Body Thermal Radiation Pressure Acting on Spacecraft," *Journal of Guidance, Control, and Dynamics*, Vol. 40, Oct. 2017, pp. 2432–2441, 10.2514/1.G002566.

[7] H. Henninger, "Solar Absorptance and Thermal Emittance of Some Common Spacecraft Thermal-Control Coatings," Tech. Rep. NASA-BP-1121, NASA, Apr. 1984.

[8] "Standard Test Method for Solar Absorptance, Reflectance, and Transmittance of Materials Using Integrating Spheres," Tech. Rep. E903.35850, ASTM.

[9] "Determination of Emittance of Materials Near Room Temperature Using Portable Emissometers," Tech. Rep. C1371-15, ASTM.

[10] D. G. Gilmore, *Spacecraft Thermal Control Handbook, Volume I: Fundamental Technologies*, Vol. 1. The Aerospace Press, 2 ed., 2002.

[11] T. S. Group, "SYSTEMS IMPROVED NUMERICAL DIFFERENCING ANALYZER (SINDA) : ENGINEERING-PROGRAM MANUAL," Tech. Rep. NASA-CR-134272, June 1971.